

Effects of an air curtain on the temperature distribution in refrigerated vehicles under a hot climate condition

Cong, Lin; Yu, Qinghua; Qiao, Geng; Li, Yongliang; Ding, Yulong

DOI:
[10.1115/1.4043467](https://doi.org/10.1115/1.4043467)

License:
None: All rights reserved

Document Version
Peer reviewed version

Citation for published version (Harvard):
Cong, L, Yu, Q, Qiao, G, Li, Y & Ding, Y 2019, 'Effects of an air curtain on the temperature distribution in refrigerated vehicles under a hot climate condition', *Journal of Thermal Science and Engineering Applications*, vol. 11, no. 6, 061010. <https://doi.org/10.1115/1.4043467>

[Link to publication on Research at Birmingham portal](#)

General rights

Unless a licence is specified above, all rights (including copyright and moral rights) in this document are retained by the authors and/or the copyright holders. The express permission of the copyright holder must be obtained for any use of this material other than for purposes permitted by law.

- Users may freely distribute the URL that is used to identify this publication.
- Users may download and/or print one copy of the publication from the University of Birmingham research portal for the purpose of private study or non-commercial research.
- User may use extracts from the document in line with the concept of 'fair dealing' under the Copyright, Designs and Patents Act 1988 (?)
- Users may not further distribute the material nor use it for the purposes of commercial gain.

Where a licence is displayed above, please note the terms and conditions of the licence govern your use of this document.

When citing, please reference the published version.

Take down policy

While the University of Birmingham exercises care and attention in making items available there are rare occasions when an item has been uploaded in error or has been deemed to be commercially or otherwise sensitive.

If you believe that this is the case for this document, please contact UBIRA@lists.bham.ac.uk providing details and we will remove access to the work immediately and investigate.

1

2

3

4

5 **Effects of air curtain on temperature distribution in refrigerated**

6 **vehicles under a hot climate condition**

7

8

9 Lin Cong¹, Qinghua Yu^{1,*}, Geng Qiao², Yongliang Li¹, Yulong Ding¹

10

11

12 ¹ *Birmingham Centre for Energy Storage, School of Chemical Engineering, University of*

13 *Birmingham, Birmingham B15 2TT, United Kingdom*

14 ² *Global energy interconnection research institute Europe GmbH, Kantstraße 162, Berlin, 10623,*

15 *Germany*

*Corresponding author. Tel.: +44 (0) 121 414 5965, Email: Q.Yu@bham.ac.uk (Q. Yu)

Abstract

Refrigerated vehicle plays an essential role in the cold-chain applications. It directly affects the quality and shelf life of specialized perishable goods. However, the cold energy dissipation caused by natural convection through an open door during partially unloading breaks the isothermal cold environment and notably elevates the air temperature inside the refrigerated container. This temperature rise is harmful to the remaining food. In this study, an air curtain was introduced near the container doorway to attempt to reduce the cold energy dissipation caused by partially unloading. A numerical model was established to explore the effects of the key parameters of the air curtain such as the airflow rate, nozzle width and jet angle on the air flow and temperature evolution inside the refrigerated container after the door is opened. The numerical results show that the key parameters need to be tailored to form a stable and effective air curtain for preventing the internal cold energy loss or external hot air invasion. An effective and stable air curtain was formed to make the inner air temperature only increase by about 3 °C from the initial temperature of 5 °C after the door was opened, when the jet velocity was set to 2 m/s, the nozzle width was set as 7.5 cm, and the jet angle was set between 0° and 15°. This work can offer significant guidance for the introduction of an effective air curtain in a refrigerated vehicle to avoid failure of cold-chain transportation.

Keywords: Refrigerated vehicle; Numerical simulation; Air curtain; Temperature evolution.

1. Introduction

Cold-chain transportation by refrigerated vehicles is rapidly expanding in the agriculture and food sectors over the last decades because it is crucial to food safety and quality. It also contributes substantially to energy consumption and greenhouse gas emissions. Meanwhile, refrigeration equipment in the vehicles has lower efficiencies than stationary applications because of the wide operating condition range and constraints in available weight and space. The two aspects make the cold-chain transportation industry face considerable challenges in reducing the energy consumption and greenhouse gas emissions of refrigerated vehicles [1]. Due to its strict requirement for temperature distribution control of transported goods governed by the legislation about storage and transport of perishable goods, the strategy to reduce energy consumption must take the temperature control as a prerequisite [2]. Tassou et al. [1] stated that frequently opening the door for partially unloading goods is the major cause of the heat loss and the cold energy dissipation, which results in not only unwanted energy consumption increase but also degradation of perishable goods. Introducing an air curtain at the doorway of refrigerated vehicles is considered an effective solution to the issue caused by frequently opening door [3]. This method can also reduce the required rated power of refrigeration equipment and losses arising from frequent on/off cycling of the equipment.

A number of studies have been devoted to the performance of the air curtains in various applications in recent years. Liebers et al. [4] experimentally investigated the reduction of the heat losses through open doors by installing air curtains in urban buses. They found that the air curtains had a notable effect on the heat exchange process. A major reduction was achieved on the energy losses for more than 20 seconds after the door was opened. Besides experimental studies, the computational fluid dynamics (CFD) has been considered a powerful tool and widely

used in the study of air flow [5, 6]. Ye et al. [7] numerically studied the ability of the air curtain to prevent infiltration of outdoor cold air into a large space building in winter. The results showed that the use of air curtain effectively reduced the outdoor air infiltration and maintained the indoor heat comfort. Belleghem et al. [8] established a CFD model to study in detail the performance of a vertical single-jet air curtain installed at the doorway of a refrigerated storage room. They stated that the air curtain achieved maximum effectiveness as the air outlet momentum can ensure that the air jet stably reached the opposite side. In an optimal condition, air curtain reduced the heat transfer between indoor and outdoor to 20% with respect to the case without an air curtain. More researches were conducted on the performance of an air curtain in refrigerated display cabinets [9]. Cao et al. [10, 11] established an effective strategy for optimizing an air curtain of an open vertical refrigerated display cabinet. With the optimum parameters, the cooling loss was decreased by 19.6% whilst the energy consumption was reduced by 17.1%. Chang et al. [12] demonstrated that the temperature of food packages in a refrigerated display cabinet decreased by 0.2~1.1 °C when the outlet velocity of the air curtain increased by 0.15m/s. Laguerre et al. [13] stated that the load temperature was reduced by increasing the turbulence of the air curtain whereas the energy consumption increased. Amin et al. [14, 15] used a tracer gas technique to determine the relationship between the infiltration of outside air into the display cabinet and important variables, such as jet exit Reynolds number, offset angle, throw angle and turbulence intensity. Several studies have also been conducted on the performance of an air curtain in a refrigerated truck. Tso et al. [3] experimentally compared the heat transfer characteristics inside a refrigerated truck in the following three cases: without an air curtain, with a plastic strip curtain and with an air curtain. They reported that the case with an air curtain achieved the least temperature rise from an initial temperature and considerable

energy savings within 2 min after the door was opened compared to the other two cases. Liang et al. [16] numerically investigated the effects of the export velocity of an internal-suction-type air curtain on its heat preservation performance in a refrigerated truck when the door was opened. The truck was equipped with a container measuring $3.1\text{ m} \times 1.52\text{ m} \times 1.52\text{ m}$ (length \times width \times height). The results suggest that air curtain can offer the best heat preservation performance at a suitable export velocity (0.5 m/s). When the velocity is higher, it would aggravate the air circulation and increase energy consumption. However, the average temperature inside the container was increased by 9 °C when the door was opened for 1 min at the optimum export velocity of the air curtain. It implies that the ability of the suction-type air curtain is limited and the air curtain needs to be redesigned to achieve better results.

Although the air curtain plays a critical role in cold energy preservation inside an open cavity or container by cutting off the heat and mass exchange between inside and outside, its performance and design in the application of refrigerated vehicles under hot climate conditions remain largely unaddressed. Particularly, the following issues have not been addressed in the literature: a) the air flow and temperature evolution inside the refrigerated container with or without a jet-type air curtain after the door is opened; b) the effects of key parameters of air curtain on the cold energy preservation or temperature inside the refrigerated container, such as jet velocity, nozzle width and jet angle. To cover the unaddressed problems, a numerical model was established in this study to reproduce the transient air flow and temperature evolution for a typical refrigerated container without or with an air curtain after the door is opened. The model was developed in commercial CFD software Fluent 18.2 and validated by comparing with previous numerical studies. Based on the model, the effects of key parameters of the air curtain were explored and elaborated. The suitable parameter ranges to ensure the stability and

effectiveness of the air curtain were then obtained. This study provides a better understanding and comprehensive guidance on the energy-saving design of air curtains for refrigerated vehicles. To the authors' knowledge, this study is the first of this kind for refrigerated vehicles with air curtains.

2. Numerical model

2.1. Model setup and governing equations

The schematic diagram of a typical commercial refrigerated vehicle/container is illustrated in Fig. 1. The container has dimensions of 4.2 m \times 2.2 m \times 2.2 m (length \times width \times height) with an insulation wall layer of 0.1 m thickness. It is assumed that the perishable goods and container are pre-cooled to the desired temperature (5 °C). Goods were placed in the left domain inside the refrigerated container and the right domain occupied with the stationary air of 5 °C when the door is closed. The ambient temperature outside the container was set to 35 °C. The thermophysical properties of air and pre-cooled goods are listed in Table 1.

Table 1 Thermoproperties of air and pre-cooled goods.

| | Air | Pre-cooled goods |
|------------------------------|--------------------------|------------------|
| Density (kg/m ³) | Incompressible-ideal gas | 540 |
| Specific heat (j/kg K) | 1006.43 | 2193 |
| Thermal conductivity (w/m K) | 0.0242 | 0.14 |
| Viscosity (kg/m s) | 1.7894e-5 | |

The dashed lines in the sectional view in Fig. 1 show the location of the door of the container. For the container equipped with an air curtain, grilles are installed at both the top and bottom of

the doorway. When the door opens, the cold air (set as 5 °C) is ejected from the top grille (i.e. nozzles) and returns through the bottom grille, and a jet-type air curtain is therefore formed at the open doorway. The cold air can be supplied by a refrigerated system or a high-pressure air storage tank with a throttling device. The latter can respond to the door opening more rapidly and efficiently. The cold air can also be a reused by-product from the cryogenic applications, such as liquid air energy storage or cold energy recovery during regasification of liquefied natural gas. The moment when the door is opened is regarded as the initial time of simulations, i.e. $t=0$.

The air at atmospheric pressure is considered an ideal gas and Newtonian fluid. The temperature difference between the air outside and inside the container leads to a horizontal gradient of air density. The density gradient combined with the action of gravity induces natural convection of air and accompanied a heat transfer when the door is opened. Gravity was considered in this simulation along the opposite direction of the Y axis. The addition of air curtain introduces forced convection of air. The transient mixed convection of air is governed by the conservation equations of mass, momentum and energy, which can generally be written as follows, respectively:

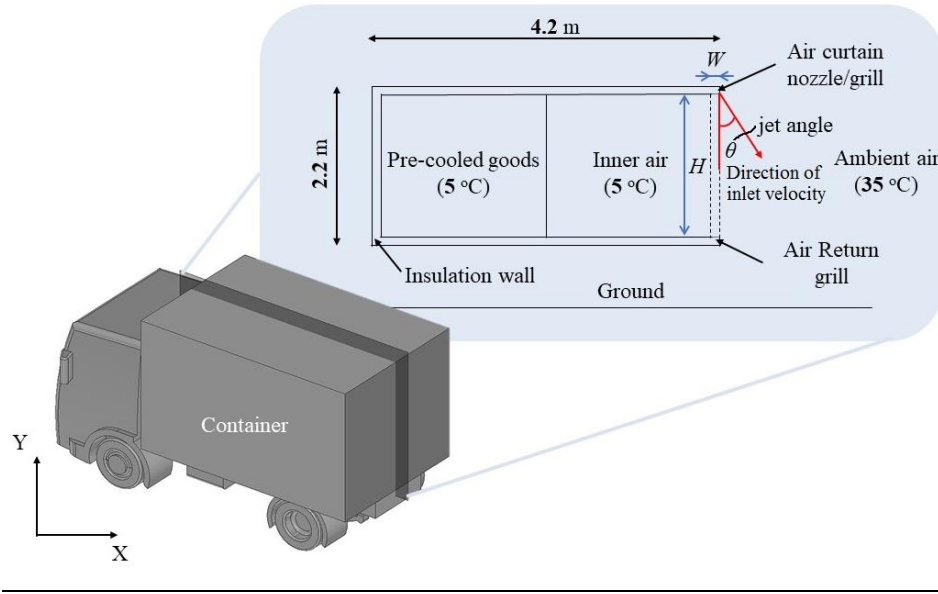
$$\frac{\partial u_i}{\partial x_i} + \nabla \cdot (\rho \vec{V}) = 0 \quad (1)$$

$$\rho \frac{\partial u_i}{\partial t} + \rho \frac{\partial u_i u_j}{\partial x_j} = -\frac{\partial p}{\partial x_i} + \rho g_i + \frac{\partial}{\partial x_i} \left[\mu \left(\frac{\partial u_i}{\partial x_j} + \frac{\partial u_j}{\partial x_i} \right) - \rho \overline{u'_i u'_j} \right] \quad (2)$$

$$\frac{\partial T}{\partial t} + u_i \frac{\partial T}{\partial x_i} = \frac{\partial}{\partial x_i} \left(\alpha \frac{\partial T}{\partial x_i} - \overline{u'_i T'} \right) \quad (3)$$

where ρ , t , u_i , p , g_i , μ , c_p , T , α denote the density (kg/m³), time (s), velocity (m/s), pressure (Pa), gravity acceleration (m/s²), dynamic viscosity (Pa·s), specific heat (J/kg·K), temperature (K) and thermal diffusivity (m²/s), respectively.

141



142

143 **Fig. 1.** Schematic of refrigerated vehicle and container (sectional view) with an air curtain.

144

145 The computational domain should be extended from the container towards outside. The
 146 ground is treated as the bottom boundary of the extended domain, while the boundaries in other
 147 directions are extended far enough until their positions have little or no influence on the air
 148 motion and temperature distribution inside the cavity. The temperature is kept at 35 °C and the
 149 air velocity is zero at the ground, while the temperature is also kept at 35 °C and the shear stress
 150 is zero at the other extended hypothetical boundaries. Adiabatic and non-slip boundary
 151 conditions are assumed at both the internal and external surfaces of the insulation wall layer.
 152 Temperature continuity and heat flux conservation are applied at the interface of the pre-cooled
 153 goods/air in the numerical simulations. The velocity boundary is given at the air curtain
 154 grille/nozzles, where the inlet air velocity (v) varies from 0 m/s to 4m/s. The pressure boundary
 155 is given at the air return grille. Our preliminary simulations indicate that the pressure value has
 156 little effect on the air curtain. To avoid consuming excessive power to maintain the pressure at

the air return grille, the pressure is set as 0.9 bar which is close to the atmospheric pressure. The inner height of the container, the nozzle width and the jet angle are denoted by H , W and θ . The definition of the jet angle is the angle between the air velocity direction at the nozzle and the opposite direction of the Y axis. The angle is negative when the air velocity tilts inwards. In addition, the non-dimensional parameters such as Reynolds number ($Re = \rho v W / \mu$) and relative nozzle width (W/H) is introduced in the paper to extend the applicability of the study.

Since every cross-section of the container parallel with the cross-section as shown in Fig. 1 has the same boundary conditions except for the cross-section close to the side wall of the container, their flow patterns and temperature distributions should be nearly the same. In order to save computational resources, a two-dimensional (2D) model based on the cross-section as shown in Fig. 1 is adopted for the simulations in this study. The simulations were carried out through the commercial CFD software Fluent 18.2, which is based on the finite volume method. The SIMPLE scheme was selected as the solving method. The standard $k - \varepsilon$ model was employed to account for turbulent behaviour of air convection [17, 18]. The second order upwind type was used to discretize momentum and energy equations. The convergence criteria were that the residuals of continuity, momentum and energy equations at each time step achieved 10^{-3} and 10^{-3} and 10^{-6} , respectively. Once the convergence criteria were met at each time step, the transient solutions were obtained. The time step was set as 0.2 s. The velocity and temperature of air were calculated within one minute after the door is opened.

2.2. Independent test of computational domain and grids

The extended computational domain with structural grids is shown in Fig. 2. The structural grids are generated by the meshing software ICEM with refinement in the regions near the

doorway and the solid/fluid interfaces, where the velocities and temperatures steeply varied. Firstly, the independent test of the extended computational domain was conducted based on four different computational domains with the sizes of 10 m \times 5 m, 13 m \times 5 m, 13 m \times 7 m and 16 m \times 9 m in length \times height. The similar grid resolution was employed for the four computational domains. The predicted average air temperatures inside the container under the four extended computational domains are summarized in Table 2. It can be found that the average air temperature difference inside the container between the third and fourth computational domains is less than 0.3 °C. Therefore, the further simulations in this study were accomplished under the third computational domain (i.e. 13 m \times 7 m). Secondly, the independence of the grid was examined on the basis of four different grid sets with about 63,000, 75,000, 86,000 and 98,000 cells. The predicted average air temperatures inside the container under the four grid sets are also summarized in Table 2. It can be seen from this table that the difference in the average air temperature inside the container is less than 0.2 °C between the third and fourth grid sets. Thus, the following simulations in this study were accomplished under the third grid set (i.e. 86,000 cells). The independent tests of the computational domain and grids provide a good trade-off between computation accuracy and time. The monitoring points of temperatures are also displayed in Fig. 2. One is located at the air-goods interface and three points labeled by 1, 2, and 3 are located outside the container. Point 2 is located at the middle position of the doorway along the Y axis and at 0.5 m away from the doorway along the X-axis. Point 1 and Point 3 are located at 0.5 m above Point 2 and at 0.5 m on the right of Point 2, respectively. Besides, the average air temperature inside the container was also monitored.

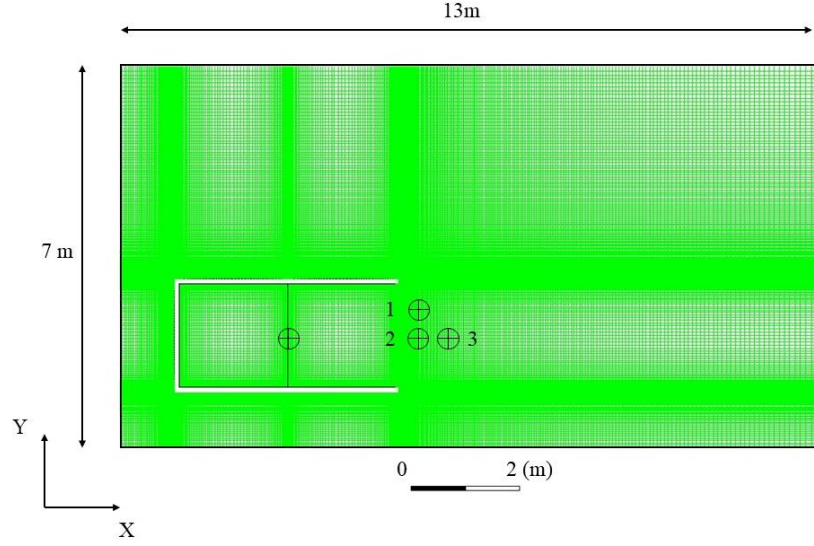


Fig. 2. The computational domain, grids and the position of the monitored points marked by \oplus .

Table 2 Results of the independent test of computational domain and grids for average air temperature (\bar{T}) inside the container at $t = 30$ s.

| Domain size | \bar{T} (°C) | Difference (°C) | Grid number | \bar{T} (°C) | Difference (°C) |
|-------------------|----------------|-----------------|-------------|----------------|-----------------|
| 10 m \times 5 m | 6.50 | - | 63,000 | 6.98 | - |
| 13 m \times 5 m | 7.32 | 0.82 | 75,000 | 7.51 | 0.53 |
| 13 m \times 7 m | 7.86 | 0.54 | 86,000 | 7.86 | 0.35 |
| 16 m \times 9 m | 8.08 | 0.22 | 98,000 | 7.97 | 0.11 |

2.3. Model validation

In order to validate the reliability of the established numerical model, the numerical simulation was carried out for an open cavity with the same geometrical configurations and thermal boundary conditions as shown in the work of Juárez et al [19]. The top and bottom horizontal walls of the open cavity was adiabatic, while its left vertical wall was kept at a constant temperature T_h . The right side of the cavity was open to the surrounding. The surrounding fluid interacting with the cavity was at a constant temperature T_l , which was lower than T_h . The temperature difference would induce natural convection of the surrounding fluid,

which is similar to the situation of the refrigerated container when the door is opened in the present study. The comparison of results obtained by the present model with those reported by Juárez et al [19] is presented in Fig. 3(a). The results are the dimensional temperature profiles along the dimensional coordinate X at the dimensional coordinate $Y=1.5$ for dimensionless temperature difference $\alpha = 0.3$ and 1.3 when the Rayleigh number is 10^4 . It can be seen from Fig. 3(a) that the results obtained by the present model agree well with those reported by Juárez et al [19] for both two different dimensionless temperature differences. Therefore, the established model proves to be valid. In order to demonstrate the accuracy of 2D simulations, a 3D simulation was carried out for the case with a jet velocity of 2 m/s and a nozzle width of 10 cm. The comparison of the average air temperature inside the container between 2D and 3D simulations is shown in Fig. 3(b). It can be found that the average temperature obtained by 3D simulation is slightly lower than that obtained by 2D. It should be attributed to the effect of the side wall of the container, which reduces the velocity of hot air flowing into the container. Even so, they have the same evolution tendency and the small temperature deviation (<0.5 °C) between 2D and 3D simulations is acceptable. It implies that the 2D simulations adopted in this paper can accurately capture the flow and heat transfer characteristics in and near the container with an air curtain.

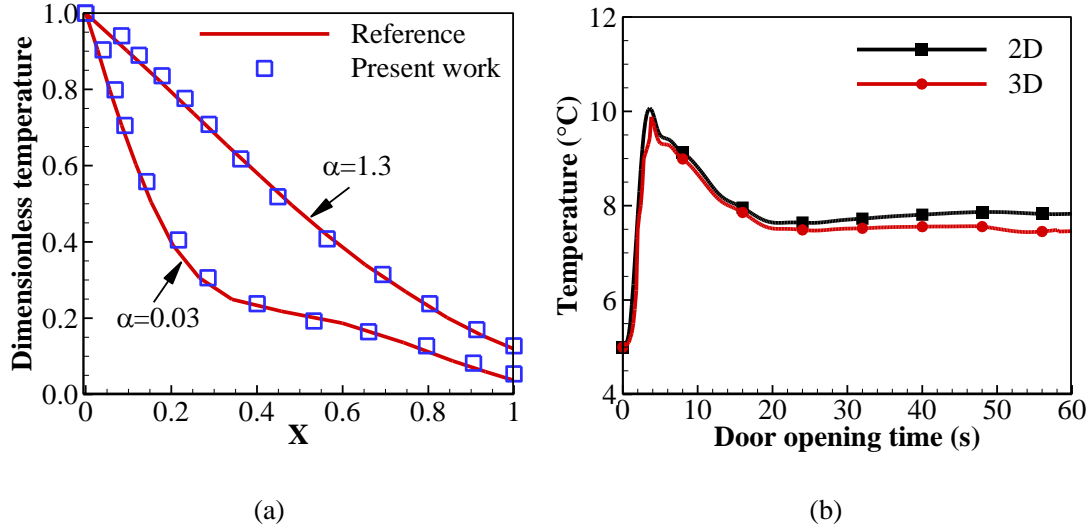


Fig. 3. (a) Validation of the present numerical model with results reported by Juárez et al [19]; (b) Comparison of the average air temperature in the container between 2D and 3D simulations.

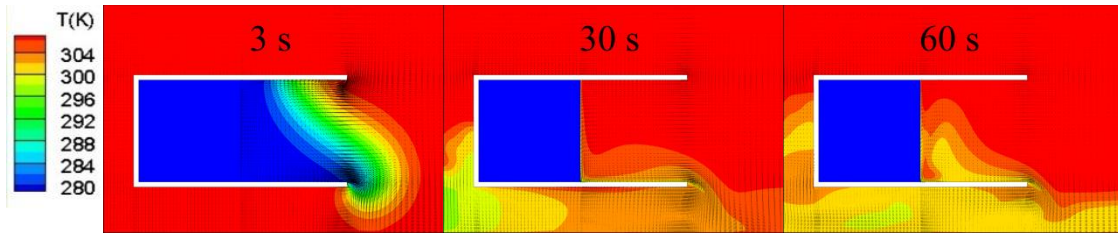
3. Result and Discussion

Based on the validated numerical model, the effects of jet velocity, nozzle width and jet angle of the air curtain on the evolution of the velocity and temperature inside the container and near the doorway were explored and elaborated respectively.

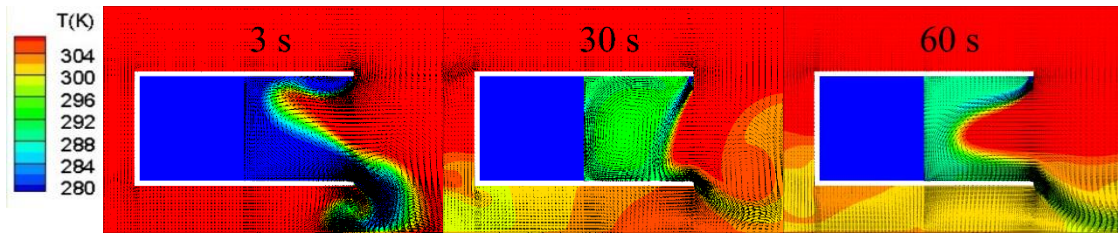
3.1. Effects of jet velocity

Fig. 4 illustrates the evolution temperature distribution and air flow pattern inside and near the container with different jet velocities (0 m/s, 1 m/s, 2 m/s and 4 m/s) of the air curtain within 1 minute after the door is opened. In all the four scenarios the air nozzle has a width of 10 cm and the air jet angle is 0 (i.e. vertical jet). It is well known that when the refrigerated container door is opened without an air curtain, hot air outside will fill into refrigerated space immediately while the inner cold air will flow outward due to the temperature difference. As is illustrated in Figure 4(a), the situation is well reproduced. After opening the door, the hot air outside is invading inward through the ceiling of the container massively, while the cold air inside is

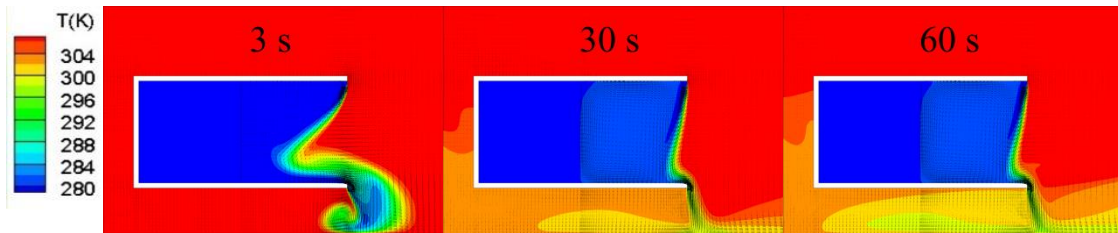
flowing outward through the bottom of the open doorway. The hot air almost occupies the whole refrigerated space at 30 s when the air curtain does not exist. The hot air continues infiltrating afterward and absorbing cold of the goods directly.



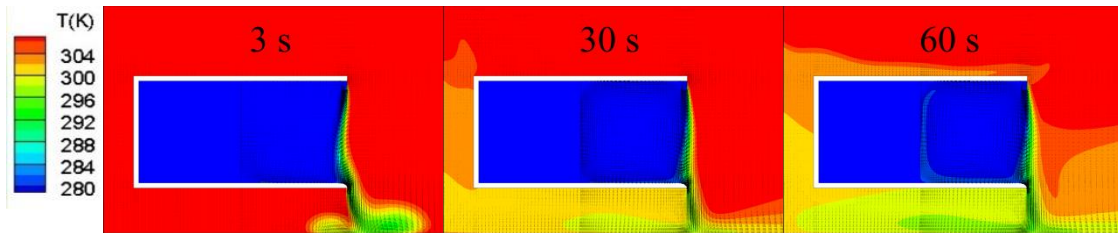
(a)



(b)



(c)



(d)

Fig. 4. The temperature and velocity distribution at 3 s, 30 s and 60 s after the door is opened when the air jet velocity of air curtain is (a) 0 m/s, (b) 1 m/s, (c) 2 m/s and (d) 4 m/s.

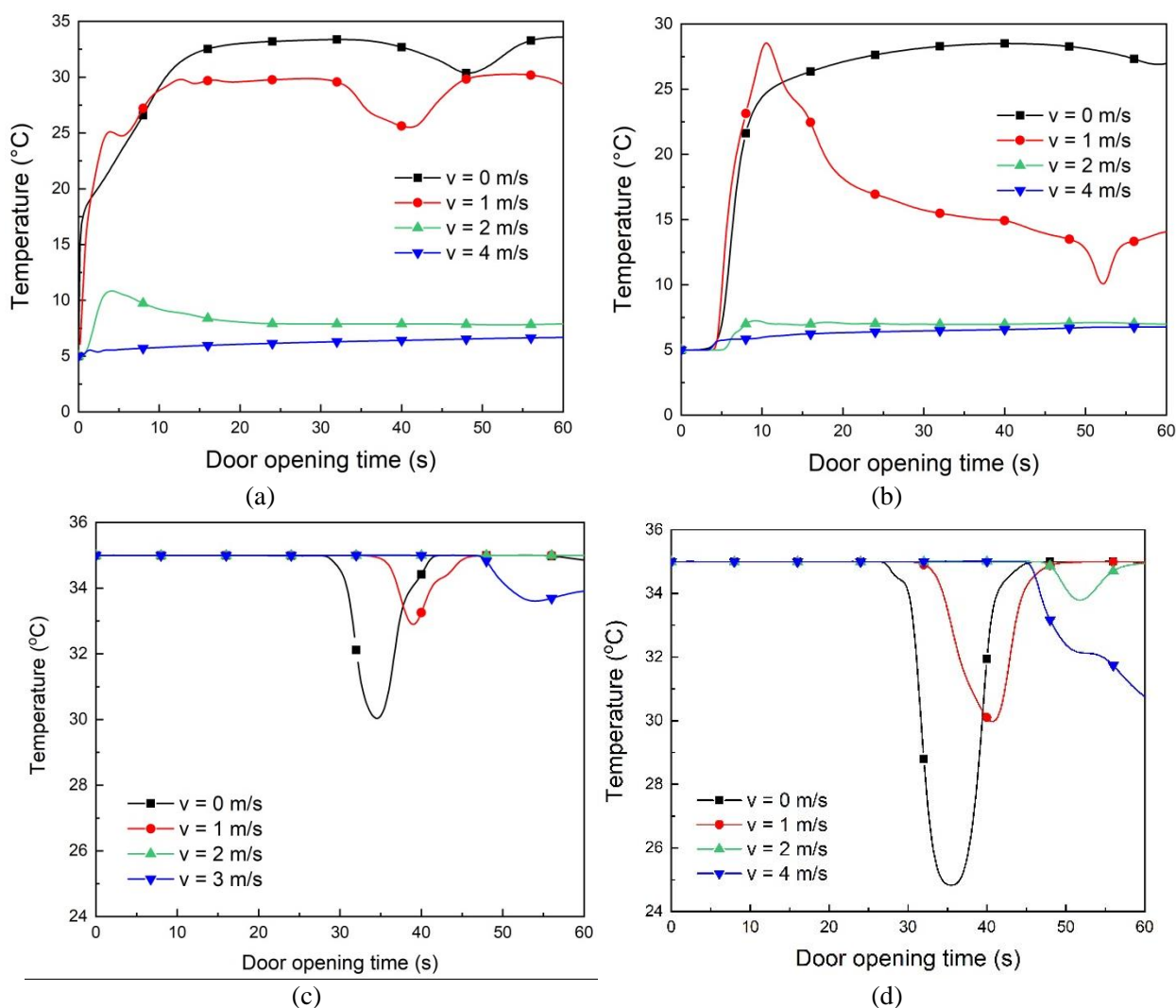
With the help of the air curtain, the hot air infiltration into the container decreases in various degrees with different air jet velocities as illustrated in Fig. 4(b-d). Generally, a larger airflow rate exhibits better insulation ability to the hot air infiltration. For the jet velocity of 1 m/s, the air curtain is unstable and cannot effectively prevent the infiltration of outer hot air. From 3 s to 30 s, the air curtain moves outward and tends to be stabilized. It becomes concave inward again at 60 s. In case of the temperature difference between inside and outside the container, the jet velocity of 1 m/s cannot provide a stable barrier between the inner cold air and outer hot air. The temperature rise is lower than that without an air curtain, though the inner air temperature increases significantly at 60 s. When the jet velocity increases to 2 m/s, the air curtain touches the bottom of the container at 30 s and maintains the shape and position stably afterward. Therefore, the infiltration of outer hot air is effectively blocked and the inner air temperature rise is effectively suppressed. When the jet velocity is further increased to 4 m/s, the improvement in the obstruction ability to the infiltration of outer hot air and suppression of temperature rise is very limited.

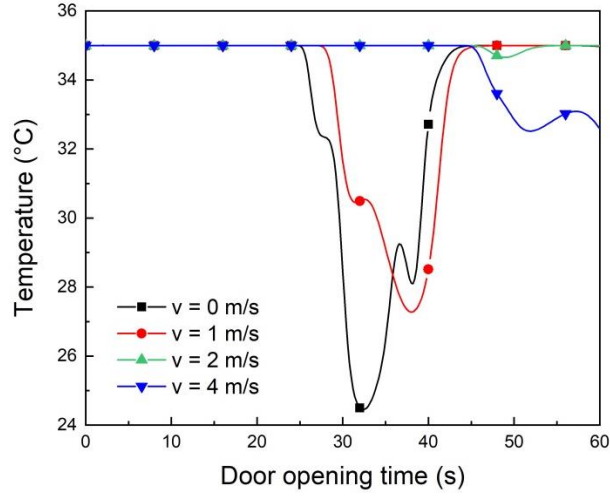
The temperature evolutions of the monitored points and surface are illustrated in Fig. 5. Various air jet velocities lead to significant differences in temperature evolutions. As is shown in Fig. 5(a), without an air curtain ($v = 0$ m/s), the average temperature of inner air increases to about 33 °C within 20 s after the door is opened and is maintained at this level with small fluctuations; in the case with the jet velocity of 1 m/s, the average temperature also sharply increases to about 29 °C within 20 s and is also maintained at this level with small fluctuations; when the jet velocity reaches 2 m/s, the average temperature smoothly increases from initial temperature to about 12 °C and then decreases back to about 7.9 °C. When the jet velocity further increases to 4 m/s, the average temperature has a minimum increment of about 6.5 °C within 60 s

among the four jet velocities. Although the jet velocity increases by twice from 2 m/s to 4 m/s, the average temperature rise only decreases by about 1.4 °C. The temperature at the goods-air interface directly reflects the risk of quality degradation of goods. Fig. 5(b) displays the temperature evolution of the monitoring point at the goods-air interface. For the jet velocity of 1 m/s, the temperature at the interface vibrates acutely within 1 min and even increases to a higher value than that without air curtain within 13 s. This is due to the convection enhancement caused by the unstable air curtain. When the jet velocity is increased to 2 m/s, the temperature at the interface slightly increase and is maintained at about 6.5 °C after 20 s. Thus, the temperature rise at the interface is also markedly reduced at $v = 2$ m/s compared to that without air curtain. When the jet velocity is further increased to 4 m/s, the improvement on temperature preservation is limited. The temperature of the monitoring point outside the container can be used to indicate the cold loss. Figs. 5(c-e) present the temperature evolution at the different monitoring points (Points 1, 2 and 3) outside the container. It can be seen that the change tendency of the temperature fluctuation amplitude with the jet velocity is the same at all the three monitoring points whilst the evolution patterns of the temperature at all the three monitoring points are similar for each jet velocity. The lower the temperature at the monitoring point outside the container is, the larger the cold loss within the container is. The cold loss is quite large when the jet velocity is lower than 1 m/s. When the jet velocity is increased to 2 m/s or 4 m/s, the cold energy loss is notably reduced, although the cold loss is slightly increased after 40 s. This part of the cold loss is provided by the air curtain. It can also be found that the cold loss at $v = 4$ m/s is larger than that at $v = 2$ m/s. Therefore, the most efficient jet velocity in this study should be 2 m/s. The above results demonstrate that introducing air curtain with precisely tailored jet velocity can help to

reduce the infiltration of outer hot air and realize decent low-temperature preservation inside the refrigerated container after the door is opened.

Further, more simulations were carried out to unveil the effect of Reynold number on the average air temperature within the container at 60 s door opening, which is shown in Fig. 6. There is a sharp temperature decline with the increase of Reynold number as Reynold number is less than 10000. When Reynold number is greater than 14000, the average temperature within the container nearly keeps constant with the increase of Reynold number. It means that the air curtain is enough to effectively maintain a low temperature within the container when Reynold number is 14000, which corresponds to the jet velocity of 2 m/s in this study.





(e)

Fig. 5. The temperature evolution within 1 min after the door is opened with different air jet velocities (v): (a) the average air temperature inside the container; (b) the temperature of monitoring point at the air-goods interface; (c-e) the temperature outside the container at Point 1, Point 2 and Point 3, respectively.

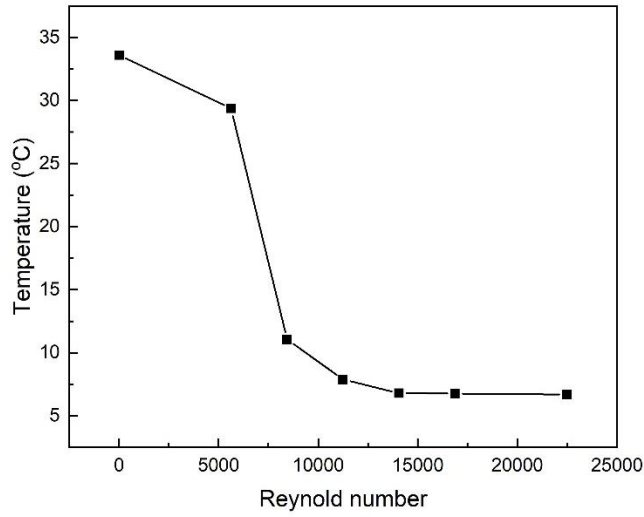
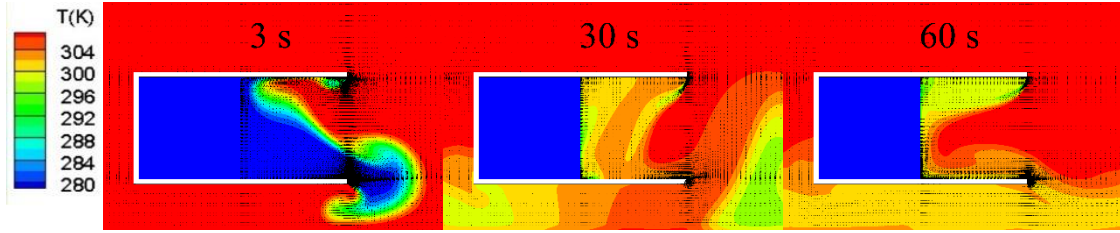


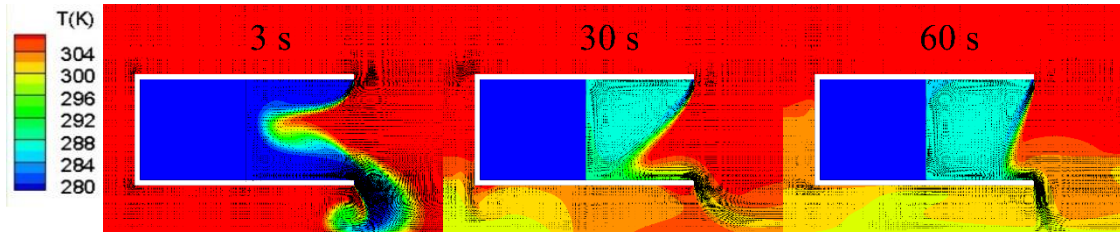
Fig. 6. Variation of the average air temperature in the container with Reynold number at 60 s after door opening.

3.2. *Effects of nozzle width*

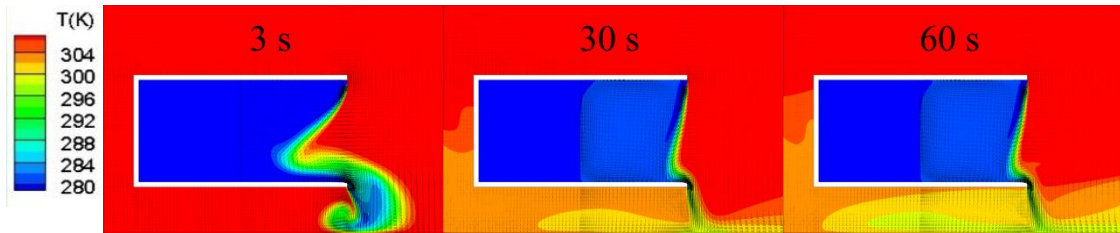
To study the influence of the nozzle width of the air curtain, the air convection and heat transfer of air curtains with nozzle widths of 1 cm, 5 cm and 10 cm were simulated and comparatively analysed. At this section, the air jet velocity was set to 2 m/s. Fig. 7 presents the transient air convection patterns and temperature distribution for different nozzle widths. It is obvious that the nozzle width significantly influences the stability of the air curtain. As is shown in Fig. 7(a), the air curtain with a nozzle width of 1 cm is too weak so that the air jet does not reach the container and the air curtain is severely concave inwards. The air curtain cannot withstand the ventilation caused by the large temperature difference between the air inside and outside the container. Within 3 s after the door is opened, a large amount of hot air invaded from the outside while the cold air continuously flows outwards. After 30 s, the hot air almost occupied the whole cold space. Within the calculating period, the air fluctuated wildly in the space. The air curtain with a nozzle width of 5 cm in Fig. 7(b) provides better temperature preservation compared to that with a nozzle width of 1 cm. A relatively stable air curtain is formed after 60 s, which prevents the infiltration of the outer hot air to some extent. However, the air curtain is still concave inwards and the air temperature inside the container still shows a noticeable rise after 60 s. When the nozzle width is further increased to 10 cm as shown in Fig. 7(c), a more stable air curtain is formed and creates a good thermal barrier to prevent the infiltration of the outer hot air, which demonstrates the best performance of all three nozzle widths.



(a)



(b)

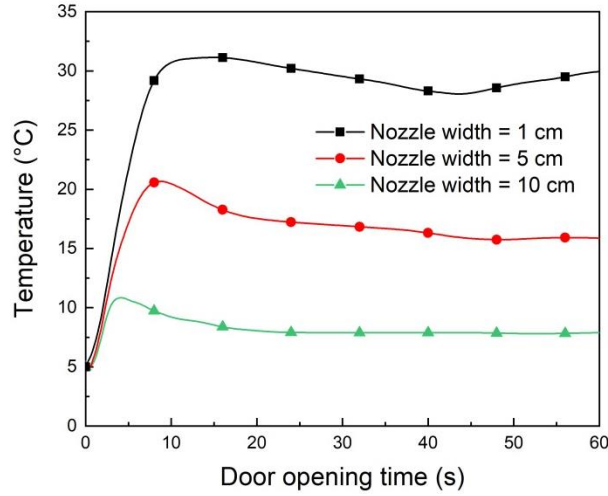


(c)

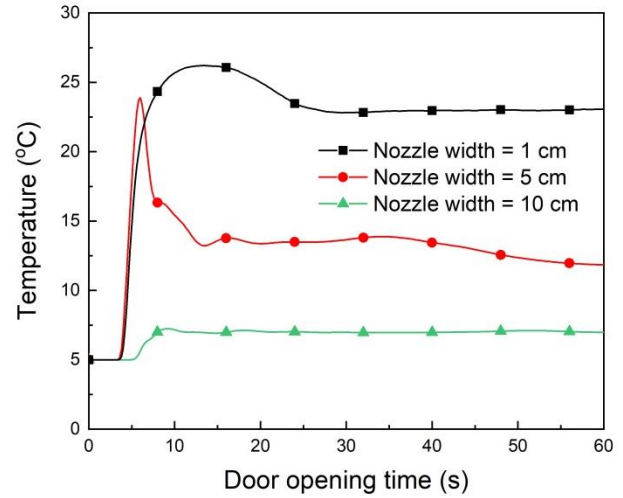
Fig. 7. The temperature and velocity distribution (3 s, 30 s and 60 s) when the nozzle widths of air curtain are (a) 1 cm, (b) 5 cm and (c) 10 cm, respectively.

The profiles of temperature evolution under different nozzle widths are summarized in Fig. 8. The evolutions of average air temperature inside the container show a similar change trend for the three nozzle widths as shown in Fig. 8(a). Generally, they first increase sharply and then decrease slowly until keeping constant. Both the increasing rate and end temperature decrease with the increase of the nozzle width. The average air temperature inside the container first arises to about 31.5 °C, 21.0 °C and 11.0 °C after the door is opened for nozzle widths of 1 cm, 5 cm

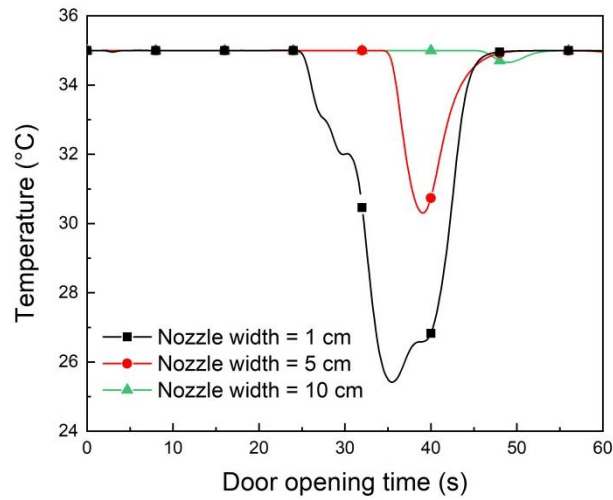
and 10 cm, respectively. Afterward, they decrease to about 30.0 °C, 16.0 °C and 7.9 °C at 60 s, respectively. The average air temperature is stabilized more quickly with the nozzle width of 10cm than other nozzle widths. The temperature evolutions of the monitoring point at the goods-air surface are shown in Fig. 8(b). When the nozzle width of the air curtain is 1 cm, the air contacting with the surface of the goods has increased the temperature to about 26 °C within 15 s and eventually maintained at about 23 °C. For the case with a nozzle width of 5 cm, this temperature increases sharply to about 24 °C within 8 seconds and eventually reduces to about 12 °C at 60 s. The air curtain with a nozzle width of 10 cm keeps a stable inner air environment from the very beginning and keeps the temperature at the goods-air interface near 6.5 °C. Fig. 8(c) shows the temperature evolution of the monitoring point 3 outside the container. It indicates that the value of the nozzle width is inversely proportional to the cold loss. Besides, a larger nozzle width delays the occurring of cold loss. For instance, the cold loss into the ambient is detected at about 25 s for the nozzle width of 1 cm, about 35 s for the nozzle width of 5 cm and 44 s for the nozzle width of 10 cm. Further, more simulations are carried out to reveal the effects of relative nozzle width on the average air temperature in the container at 60 s after door opening, as shown in Fig. 9. When the relative nozzle width is below 0.0375, the average temperature linearly and markedly decreases. When the relative nozzle width increases from 0.0375 to 0.05, the average temperature slightly decreases. It means that the air curtain is effective enough when the relative nozzle width set between 0.0375 and 0.05, which correspond to the nozzle width between 7.5 cm and 10 cm. The stable average air temperature inside the container is about 8.0 °C after the door is opened for the nozzle width of 7.5 cm.



(a)



(b)



(c)

Fig. 8. The temperature evolution within 1 min after the door is opened with different nozzle widths: (a) the average air temperature inside the container; (b) the temperature of the monitoring point at the air-goods interface; (c) the temperature of the monitoring point 3 outside the container.

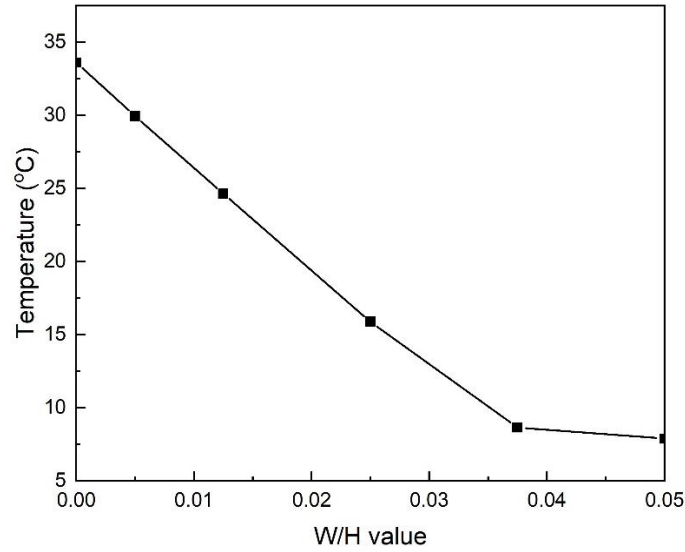


Fig. 9. Variation of average air temperature in the container with relative nozzle width (W/H) at 60 s after door opening.

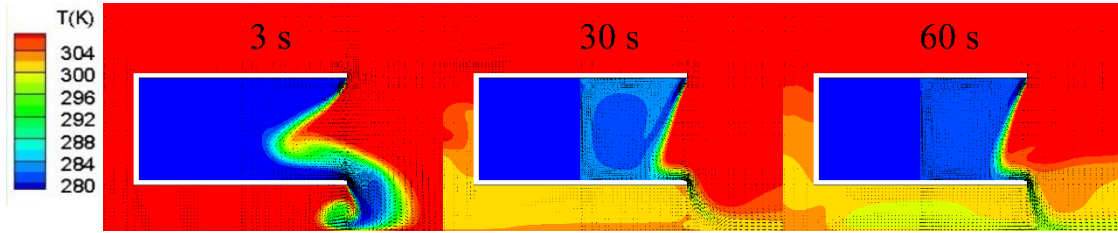
3.3. Effects of jet angle

Four different jet angles of air curtain were studied at a jet velocity of 2 m/s with a nozzle width of 10 cm. The jet direction along the negative Y-axis is defined as 0° and the jet direction towards the outside of the container is positive. The effects of jet angle were examined among -15° , 0° , 15° and 30° . Fig. 10 shows the temperature distributions under different jet angles. The jet angle causes less effect than jet velocity and nozzle width since the temperature distributions under different jet angles are similar. When the jet angle is -15° as shown in Fig. 10(a), the air curtain blows more cold energy out and entrains more hot air into the container than other cases, because it partially follows the direction of natural convection. During the pure natural convection as shown in Fig. 4(a), the buoyancy force makes the hot air flow into the container from the upper part of the doorway while the cold air flows out of the container from the lower part of the doorway. The air flow caused by the air curtain with -15° jet angle has a similar

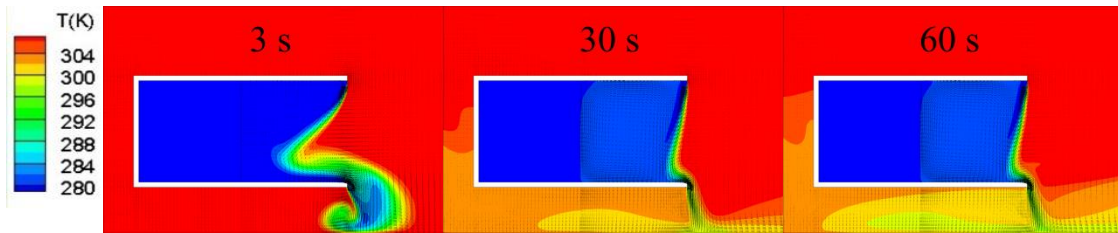
direction. Also, it provides a minimum cold space after the air curtain becomes stable at 60 s. The temperature distributions show little changes as the jet angle increases from 0° to 30° as shown in Fig. 10(b-d), except those near the air curtain. The air curtain is only concave inwards at a jet angle of 0° , while they are convex outwards near the ceiling of the container and concave inwards near the floor of the container at jet angles of 15° and 30° .

The profiles of temperature evolution with different jet angles are summarized in Fig. 11. It can be seen from Fig. 11(a) that the air curtain with a jet angle of 15° provides the best performance in preventing the infiltration of outer hot air and keeps the average air temperature at about 7.6°C . When the jet angle is decreased to 0° or increased to 30° , the average air temperature slightly increases. When the jet angle decreased to -15° , the average air temperature markedly increases to 11.5°C . For the temperature at the goods-air interface as shown in Fig. 11(b), the air curtain with a vertical jet angle (0°) provides the lowest interface temperature among the four jet angles, which is kept at about 7°C . The interface temperature with the jet angle of 15° is a little higher than the vertical jet angle with an increment of about 0.3°C . According to the temperature distributions for 0° jet angle and 15° jet angle as shown in Figs. 10(b) and 10(c), it can be seen that the air curtain for 0° jet angle tilts outwards while that for 15° jet angle exhibits an “S” shape. It implies that larger area within the container for 0° jet angle is occupied by hot air than that for 15° jet angle while more amount of cold energy for 0° jet angle is transported to the gas/goods interface. Therefore the average temperature within the container for 15° jet angle is lower while the temperature at the gas/goods interface for 0° jet angle is lower as shown in Figs. 11(a) and 11(b). Even so, the temperature difference between the two cases with 0° jet angle and 15° jet angle is quite small. From the temperature evolution of the monitoring point 3 outside the container as shown in Fig. 11(c), it can be seen that only very

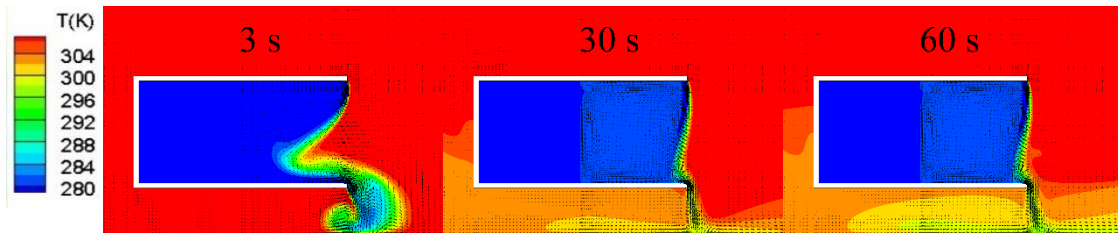
small cold loss occurs under jet angles of 0° , 15° and 30° , while the jet angle of -15° leads to markedly larger cold loss. From the above, the jet angle between 0° and 15° is a preferable choice.



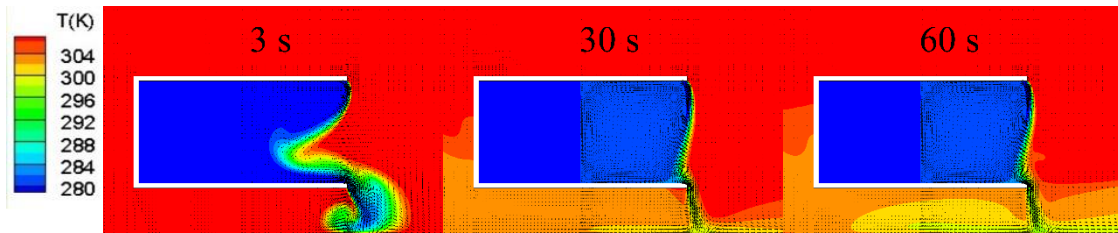
(a)



(b)



(c)



(d)

Fig. 10. The temperature and velocity distribution (3 s, 30 s and 60 s) when the jet angles of air curtain are (a) - 15° , (b) 0° , (c) 15° and (d) 30° , respectively.

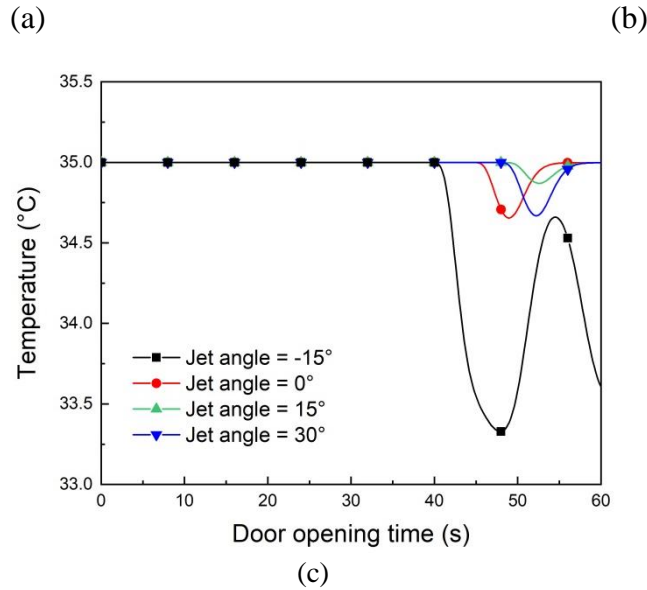
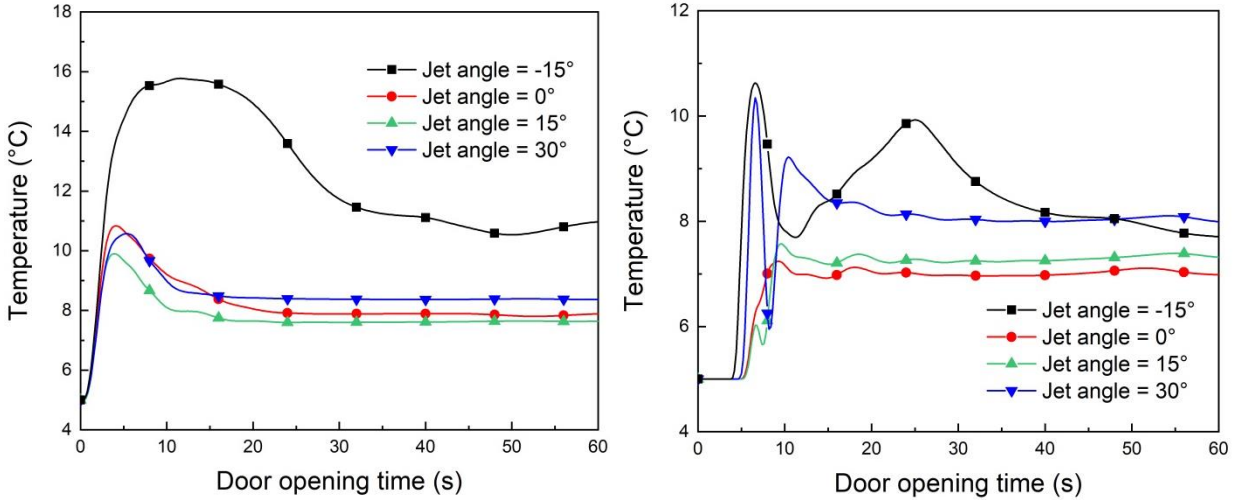


Fig. 11. The temperature evolution within 1 min after the door is opened with different jet angles: (a) the average air temperature inside the container; (b) the temperature of the monitoring point at the air-goods interface; (c) the temperature of the monitoring point 3 outside the container.

4. Conclusion

Cold-chain transportation is essential for temperature-sensitive perishable goods. In order to decrease the cold loss and suppress inner air temperature rise caused by opening the door of the refrigerated container during partially unloading, an air curtain was introduced into a refrigerated

vehicle system. Three main air curtain factors which are jet velocity, nozzle width and jet angle were evaluated with numerical simulations in this study. This work provides significant guidance for the optimal design of utilizing air curtain on refrigerated vehicles. The main conclusions are as follows: (1) The addition of an air curtain significantly decreases the cold loss within the container. (2) The jet velocity and nozzle width of air curtain provide larger influences on the air temperature distribution and cold loss inside the container than the jet angle. (3) With an increasing jet velocity, the cold loss decreases. When the jet velocity increases to some certain value, its further increase can only provide a very limited improvement in reduction of cold loss and preservation of low temperature but lead to low efficiency. (4) A stable and effective air curtain can be obtained by precisely tailoring the key parameters to keep the inner air temperature rise below 3 °C. The preferable parameter combination in this study was a jet velocity of 2 m/s, a nozzle width of 7.5 cm and a jet angle between 0° and 15°. Two non-dimensional parameters, Reynolds number and relative nozzle width, are introduced to extend the applicability of this study.

Acknowledgement

The authors would like to acknowledge the financial support of the Engineering and Physical Sciences Research Council (EPSRC) of the United Kingdom (Grant Nos. EP/N000714/1 and EP/N021142/1).

References

- [1] S.A. Tassou, G. De-Lille, Y.T. Ge, Food transport refrigeration – Approaches to reduce energy consumption and environmental impacts of road transport, *Applied Thermal Engineering*, 29 (2009) 1467-1477.
- [2] Y. Wild, Transport and storage of perishable and temperature sensitive products, Ingenieurbüro GmbH, Berlin, 2015. <https://iumi.com/images/Berlin2015/3Pressies/1609_Dr_Wild.pdf>
- [3] C.P. Tso, S.C.M. Yu, H.J. Poh, P.G. Jolly, Experimental study on the heat and mass transfer characteristics in a refrigerated truck, *International Journal of Refrigeration*, 25 (2002) 340-350.
- [4] M. Liebers, D. Tretsiak, S. Klement, B. Bäker, P. Wiemann, Using Air Walls for the Reduction of Open-Door Heat Losses in Buses, *SAE International Journal of Commercial Vehicles*, 10 (2017).
- [5] Y.T. Ge, S.A. Tassou, Simulation of the performance of single jet air curtains for vertical refrigerated display cabinets, *Applied Thermal Engineering*, 21 (2001) 201-219.
- [6] J. Moureh, S. Tapsoba, E. Derens, D. Flick, Air velocity characteristics within vented pallets loaded in a refrigerated vehicle with and without air ducts, *International Journal of Refrigeration*, 32 (2009) 220-234.
- [7] H. Ye, J. Yu, B. Wang, Y. Liu, H. Guo, L. Tian, Study on the influence of air curtain barrier efficiency on infiltration air volume and temperature distribution in large space in winter, *Procedia Engineering*, 205 (2017) 2509-2516.
- [8] M.V. Belleghem, G. Verhaeghe, C. T'Joel, H. Huisseune, P. De Jaeger, M. De Paepe, Heat Transfer Through Vertically Downward-Blowing Single-Jet Air Curtains for Cold Rooms, *Heat Transfer Engineering*, 33 (2012) 1196-1206.

- [9] K.-z. Yu, G.-l. Ding, T.-j. Chen, A correlation model of thermal entrainment factor for air curtain in a vertical open display cabinet, *Applied Thermal Engineering*, 29 (2009) 2904-2913.
- [10] Z. Cao, B. Gu, H. Han, G. Mills, Application of an effective strategy for optimizing the design of air curtains for open vertical refrigerated display cases, *International Journal of Thermal Sciences*, 49 (2010) 976-983.
- [11] Z. Cao, H. Han, B. Gu, A novel optimization strategy for the design of air curtains for open vertical refrigerated display cases, *Applied Thermal Engineering*, 31 (2011) 3098-3105.
- [12] C. Zhijuan, W. Xuehong, L. Yanli, M. Qiuyang, Z. Wenhui, Numerical Simulation on the Food Package Temperature in Refrigerated Display Cabinet Influenced by Indoor Environment, *Advances in Mechanical Engineering*, 5 (2013) 708785.
- [13] O. Laguerre, S. Duret, H. Hoang, D. Flick, Using simplified models of cold chain equipment to assess the influence of operating conditions and equipment design on cold chain performance, *International Journal of Refrigeration*, 47 (2014) 120-133.
- [14] M. Amin, D. Dabiri, H.K. Navaz, Comprehensive study on the effects of fluid dynamics of air curtain and geometry, on infiltration rate of open refrigerated cavities, *Applied Thermal Engineering*, 31 (2011) 3055-3065.
- [15] M. Amin, D. Dabiri, H.K. Navaz, Effects of secondary variables on infiltration rate of open refrigerated vertical display cases with single-band air curtain, *Applied Thermal Engineering*, 35 (2012) 120-126.
- [16] J.J. Liang, X.Y. Peng, Z.Q. Fu, J. Xiong, Y.L. Ye, Numerical simulation of the influence of a internally suction type air curtain to refrigerated truck's heat preservation performance, in: 2015 International conference on Applied Science and Engineering Innovation, Jinan, China, 30-31 August 2015.

524 [17] N.J. Smale, J. Moureh, G. Cortella, A review of numerical models of airflow in refrigerated
525 food applications, *International Journal of Refrigeration*, 29 (2006) 911-930.

526 [18] M. Prakash, S.B. Kedare, J.K. Nayak, Numerical study of natural convection loss from open
527 cavities, *International Journal of Thermal Sciences*, 51 (2012) 23-30.

528 [19] J.O. Juárez, J.F. Hinojosa, J.P. Xamán, M.P. Tello, Numerical study of natural convection in
529 an open cavity considering temperature-dependent fluid properties, *International Journal of*
530 *Thermal Sciences*, 50 (2011) 2184-2197.

531